

---

EFDA–JET–CP(03)01-03

Yu.F. Baranov, X. Garbet, N.C. Hawkes, B. Alper, R. Barnsley, C.D. Challis,  
C. Giroud, E. Joffrin, M. Mantsinen, F. Orsitto, V. Parail, S.E. Sharapov  
and JET EFDA Contributors

# On the link between q-profile and ITBs



# On the link between q-profile and ITBs

Yu. F. Baranov<sup>1</sup>, X. Garbet<sup>2</sup>, N. C. Hawkes<sup>1</sup>, B. Alper<sup>1</sup>, R. Barnsley<sup>1</sup>, C. D. Challis<sup>1</sup>,  
C. Giroud<sup>5</sup>, E. Joffrin<sup>2</sup>, M. Mantsinen<sup>4</sup>, F. Orsitto<sup>3</sup>, V. Parail<sup>1</sup>, S. E. Sharapov<sup>1</sup>  
and JET EFDA Contributors

<sup>1</sup>EURATOM/UKAEA Fusion Association, Culham Science Centre, Abingdon, OXON, OX14 3DB, UK

<sup>2</sup>Association Euratom-CEA, CE de Cadarache, F-13108, St Paul lez Durance, France.

<sup>3</sup>Associazione EURATOM-ENEA sulla Fusione, C.R. Frascati, Frascati, Italy.

<sup>4</sup>Helsinki University of Technology, Association Euratom-Tekes, Finland.

<sup>5</sup>FOM instituut voor plasmafysica Rijnhuizen P.O. Box 1207, 3430 BE Nieuwegein, The Netherlands.

\*See Annex of J. Pamela et al., "Overview of Recent JET Results and Future Perspectives",

Fusion Energy 2000 (Proc. 18th Int. Conf. Sorrento, 2000), IAEA, Vienna (2001).

Preprint of Paper to be submitted for publication in Proceedings of the  
EPS Conference on Controlled Fusion and Plasma Physics,  
(St. Petersburg, Russia, 7-11 July 2003)

“This document is intended for publication in the open literature. It is made available on the understanding that it may not be further circulated and extracts or references may not be published prior to publication of the original when applicable, or without the consent of the Publications Officer, EFDA, Culham Science Centre, Abingdon, Oxon, OX14 3DB, UK.”

“Enquiries about Copyright and reproduction should be addressed to the Publications Officer, EFDA, Culham Science Centre, Abingdon, Oxon, OX14 3DB, UK.”

## INTRODUCTION.

Numerous experiments were performed on JET to clarify the link between rational  $q$ , magnetic shear and ITBs, by producing internal transport barriers (ITBs) in plasmas with various  $q$ -profiles [1,2]. A reconstruction of the plasma equilibrium using the EFIT code with motional stark effect (MSE) and polarimetry constraints was verified by analysing MHD activity. Modelling of transport properties of plasmas produced in the experiment was done using the TRANSP (transport analysis), JETTO (predictive transport-micro-stability) and TRB (turbulent transport) codes. Two types of ITBs were analysed corresponding to different  $q$ -profile shapes: ITBs in a region of negative magnetic shear ( $s < 0$ ) and ITBs in the vicinity of rational  $q$  surfaces. Different models were used for the calculating the linear growth rate of micro instabilities. Calculated transport coefficients predicted by theory were compared with data deduced from the experiment.

### 1. ELECTRON HEAT TRANSPORT REDUCTION IN THE NEGATIVE MAGNETIC SHEAR REGION.

Figure 1a shows the contour plot of the parameter  $\rho_e^* = \sqrt{2m_p T_e} / e (dT_e / dR) / (B_\phi T_e)$  used to characterise an ITB in JET [3]. An ITB appears soon after the start of LHCD (Fig. 1a,b). A large  $\nabla T_e$  is sustained in the plasma core during LH and ICRF heating phases, although  $\rho_e^*$  is gradually reduced. The strong  $\nabla T_e$  region expands abruptly after NB heating starts. The evolution of the  $q$ -profile, magnetic shear  $s$  and electron thermal diffusivity  $\chi_e$  is shown in Fig.2, as computed by the TRANSP [4] code. The error bars are about  $\pm 20\%$  for  $\chi_e$  and  $\pm 15\%$  for  $q$ . The time interval covers LH, ICRF and beginning of NB heating. Large negative magnetic shear  $s$  is produced in the plasma core during LHCD. Simultaneously, electron heat diffusivity is reduced to a low level of  $\chi_e \approx 0.1 \text{ m}^2/\text{s}$  in the region of the negative  $s$ . Negative shear is sustained for a long time after the end of LHCD, although its amplitude gradually reduces. A minimum of  $\chi_e$  is located in the region of the negative magnetic shear and it experiences only a small variation during LH and ICRF heating phase. No external torque and ion heating were applied in these phases. Alfvén wave cascades analysis [5] shows that  $q_{\min}$  crosses rational values as shown in Fig.1a. Results of the reconstruction of the  $q$  profile using EFIT with MSE and polarimetry constraints [6], TRANSP and JETTO [7] modelling are in agreement with this observation. An ITB moves from the region of a finite negative  $s$  towards  $s=0$  at the time, when  $q_{\min}=2$ .

A stability analysis was done for Pulse No: 57739 (Fig.1,2) using the Weiland model [8], describing ITG/TEM instabilities and implemented in the JETTO code. The linear growth rate  $\gamma_{\text{lin}}$  for the turbulence predicted by the theory has its maximum inside ITB and it varies with time from  $2 \times 10^5 \text{ s}^{-1}$  to  $5 \times 10^4 \text{ s}^{-1}$ . Predicted  $\chi_e$  at the ITB location is well above the experimental level and the model predicts no ITB formation. The main driving force for the instability in this model is  $\nabla T_{e,i}$ , which is close to its maximum within ITB and the dependence of  $\gamma_{\text{lin}}$  on the magnetic shear is relatively weak [8].

The heat transport in plasmas with  $s < 0$  induced by the Trapped Electron (TEM) and Ion

Temperature Gradient (ITG) modes was analysed using the three-dimensional global fluid simulation code TRB [9]. This simulation predicts the formation of an electron ITB in discharges with a strong negative magnetic shear, as illustrated in Fig.3. The ITB is located in the region of  $s < 0$ . It gradually weakens, when  $s_{\min}$  increases and disappears completely when  $s_{\min} > s_{\text{crit}} \approx -0.5$ , which is close to a theory prediction for the TEM mode suppression by negative magnetic shear. Fig.4 illustrates the mechanism of ITB formation in this model for the case of  $s < -0.5$ . The thermal flux induced by fluctuations can be expressed in the form  $(2/3) \Gamma_{i,e} = \langle \tilde{p}_{i,e} \tilde{u}_r \rangle = |\langle \tilde{p}_{i,e} \rangle| |\langle \tilde{u}_r \rangle| \cos(\delta_{i,e})$ , where  $\delta_{i,e}$  is a phase shift between the radial velocity  $\tilde{u}_r$  and pressure fluctuations. The radial variation of these parameters is shown in Fig.4a,b. Notably,  $\tilde{p}_e$  has a maximum and  $\cos(\delta_e)$  a deep minimum at the ITB location  $0.3 \leq r \leq 0.35$ . A reduction in  $\cos(\delta_e)$  within ITB causes a reduction in  $\chi_e$ , which is shown in Fig.4c. The ion diffusivity  $\chi_i$  is not reduced significantly. Density fluctuations with long perpendicular wavelength ( $\lambda_{\perp}^{\text{exp}} \geq 0.1\text{m}$ ) are found to be reduced within the volume enclosed by electron ITB in the experiment [10]. However, the perpendicular wavelength for ITG and TEM modes is much smaller  $\lambda_{\perp \text{ITG,TEM}} \ll \lambda_{\perp}^{\text{exp}}$  and can not be measured by reflectometry diagnostic, available on JET [10].

## 2. ION HEAT TRANSPORT REDUCTION IN THE NEGATIVE MAGNETIC SHEAR REGION.

Statistical analysis shows that the ion ITB in JET plasmas is formed in the region of small or negative magnetic shear. Fig.5 shows the ratio of the ITG mode linear growth rate  $\gamma_{\text{ITG,lin}}$  to the plasma flow shearing rate  $\omega_{W \times B}$  as a function of magnetic shear at the location and the time of ITB formation. Weiland [8] and Rogister [11] models were used to calculate the linear growth rates  $\gamma_{\text{lin,ITG}}$ . The Rogister model describing ITG instability for a small  $s$  predicts efficient sheared flow stabilisation for  $|s| \ll 1$ . Weiland model predicts large values of  $\gamma_{\text{lin,ITG}}/\omega_{W \times B} > 1$  for all observed  $s$ . Neither model predict a turbulence stabilisation for  $s \leq -0.5$ .

An effect of the negative magnetic shear on the ion heat transport can be seen in discharges with so called ‘current hole’ [6]. Plasma temperature  $T_{e,i}$  and heat diffusivity profiles  $\chi_{e,i \text{ exp}}$ , are shown in Fig.6 for such case. Several time slices corresponding to the start of the main heating phase were selected. The diffusivities were deduced from TRANSP modelling with accuracy of  $\pm 20\%$ . The  $q$ -profiles were reconstructed using EFIT equilibrium code with MSE constraints with error bars of  $\pm 15\%$ .

The ITB criterion  $\rho_{e,i}^* \geq \rho_{\text{crit}}^*$  is fulfilled for electrons and ions for  $t \geq 4\text{s}$ . Both,  $\chi_{e,i}$  are reduced locally in the region of  $s < 0$  with  $\min(\chi_i)$  being close to the neoclassical diffusivity. The growth rate  $\gamma_{\text{lin}}$  and shearing rate  $\omega_{W \times B}$  are shown in Fig.6 as deduced from JETTO simulations with Weiland model. Obviously, the sheared plasma flow stabilisation [12] is not effective within the ITB ( $R=3.3-3.35\text{m}$ ) as the Weiland model predicts  $\gamma_{\text{lin}} \gg \omega_{W \times B}$ . This model predicts large values of  $\chi_{i,\text{model}} \gg \chi_{\text{exp}}$ . It does not predict the ion ITB formation.

The TRB code was used to calculate a stability of the ITG/TEM modes and to simulate the ion

ITB formation for the case of  $s < 0$ . The code predicted a stabilisation of the TEM mode and a reduction in the electron heat diffusivity leading to the formation of the electron barrier. ITG modes remained unstable. Predicted ion heat transport was large and no ion ITB was formed in the simulation. It should be noted that simulations using flux tube gyrokinetic code GS2 indicate an ITB formation for very small  $s < -2.5$  [13]. GS2 code simulations show that ITB formation for larger  $s$  requires sheared flow stabilisation.

### 3. ITB FORMATION IN VICINITY OF $S=0$ AND LOW ORDER RATIONAL $Q$ .

An ITB is formed in many cases in JET at the time, when  $q_{\min}$  crosses an integer number [1,2]. One such event occurs in Pulse No: 57739 at  $t = 4.2$  as illustrated in Fig.1a and Fig.2a,c. A rarefaction of the rational magnetic surfaces was discussed and analysed as a possible mechanism for ITB formation [9,14]. To investigate this formation, transport properties of two close magnetic configurations with  $q_{\min} = 2$  and 2.131 were modelled using the TRB code (Fig.7a). Calculated normalised ion pressure profiles are shown in Fig.7b. An ITB is formed in the region of  $q_{\min} = 2$ . A reduction in  $\chi_{i,e}$  is stronger in the  $q_{\min} = 2$  than for larger  $q_{\min}$  case as shown in Fig.8. An ITB is developed in both ion and electron channels. The simulation shows that it is produced due to the suppression of  $\langle \tilde{u}_r \rangle$  and  $\langle \tilde{p}_{e,i} \rangle$  fluctuations, which is stronger for wider gap between the resonant surfaces. The gap is wider in the vicinity of low order rationals [9]. The width of the gap  $\Delta$  is proportional to  $(dq/dr)^{-1}$  and  $(d^2q/dr^2)^{-1/2}$ , respectively, for linear and parabolic variation of the  $q$  inside the gap [9], which shows that small  $s$  is favourable for ITB formation.

### 4. EFFECT OF BOOTSTRAP CURRENT ON MAGNETIC SHEAR.

The bootstrap current induced in the vicinity of ITB flattens locally the  $q$  profile as shown in Fig.9. Such flattening (reduction in  $s$ ) widens a gap between the resonant magnetic surfaces and facilitates ITB sustainment. The stronger the ITB the larger the bootstrap current, which provides a feedback loop. However this effect does not provide a mechanism for ITB triggering.

### SUMMARY.

Experiments on JET and modelling show that the  $q$ -profile plays an important role in ITB formation. In particular, electron ITBs can be produced in the region of  $s < 0$  due to TEM suppression, according to TRB code simulations. The ion ITB formation in  $s < 0$  region occurs without effective flow shear stabilisation as shown by TRANSP [4] and JETTO [7] modelling. The Weiland [8], Rogister [11] models and TRB code simulations do not provide an explanation for such formation. ITB formation is observed in JET experiments, when  $q_{\min}$  crosses integer numbers. The main features of ITB formation near low rational  $q$  observed in experiments are reproduced in TRB code simulation. A key factor is small  $|s| \rightarrow 0$  in the vicinity of rational  $q$ . The bootstrap current may play a crucial role in a local reduction of  $s$  near an ITB. The Rogister model [11] predicts turbulence suppression in the vicinity of the  $s = 0$  surface.

## ACKNOWLEDGEMENTS.

This work was partly funded by the United Kingdom Engineering and Physical Sciences Research Council and EURATOM.

## REFERENCES

- [1]. C.D.Challis et al., Plasma Phys.Control. Fusion, **44** (2002)1031.
- [2]. E.Joffrin et al. Proc. 19th IAEA Fusion Energy Conf., paper EX/P1-13. (submitted to Nucl.Fusion)
- [3]. G.Tresset et al., Nucl.Fusion, **42** (2002) 520.
- [4]. Budny, R.V., et al., Nucl.Fusion **32** (1992) 429.
- [5]. S.Sharapov et al. Phys.Plasmas, **9** (2002) 2027.
- [6]. Hawkes N.,C., et al, PPCF **44** (2002) 1105
- [7]. Tala T.J.J., et al., Plasma Phys. Control. Fusion, **44** (2002)A495.
- [8]. Guo, S.C., Weiland, J., Nucl. Fusion **37** (1997) 1095.
- [9]. X.Garbet, et al., Phys.Plasmas, **8** (2001) 2793.
- [10]. Conway G.D., et al., Plasma Phys.Control.Fusion **44** (2002)1167.
- [11]. Rogister, A.L., Phys. Plasmas **7** (2000) 5070.
- [12]. Hahn T.S. et al., Phys.Plasmas, **2** (1995) 1648. to Nucl.Fusion (2002).
- [13]. Budny R., et al., Turbulence and heat and particle fluxes in JET and DIII-D ITB plasmas with highly reversed magnetic shear. This conference.
- [14]. Garbet, X., et al., Micro-stability and Transport Modelling of ITBs on JET. Submitted to Nucl.Fusion (2002).



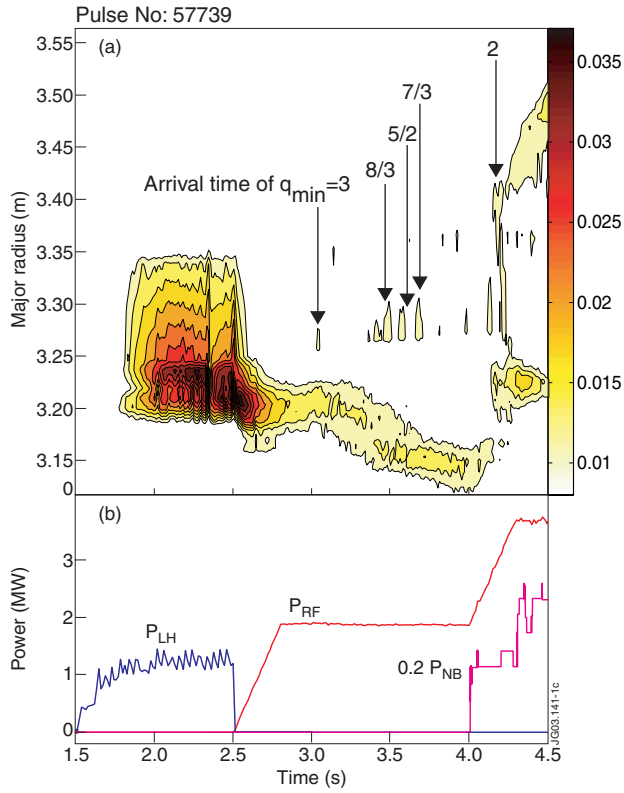


Figure 1. a)  $q^*$  contour plot and b) heating power waveform.

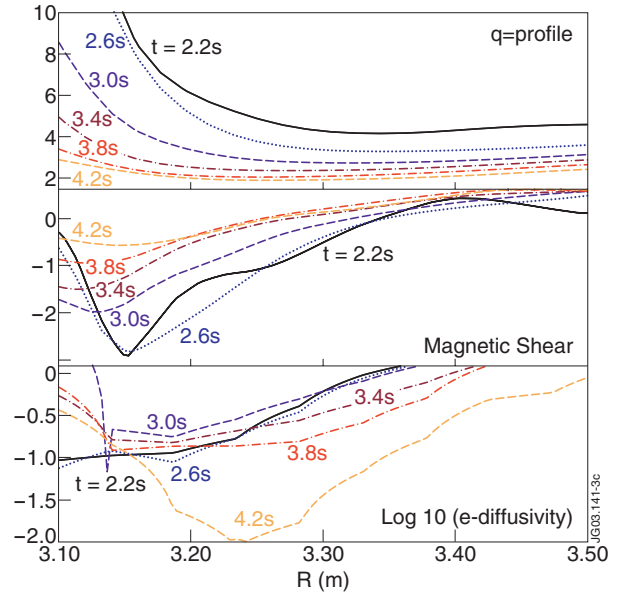


Figure 2. TRANSP modelling. Pulse No: 57739

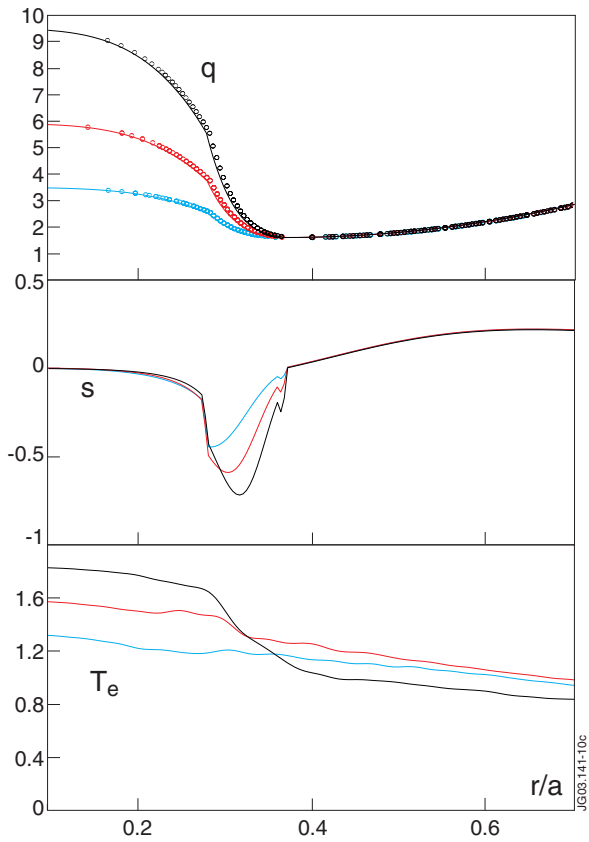


Figure 3. TRB simulations

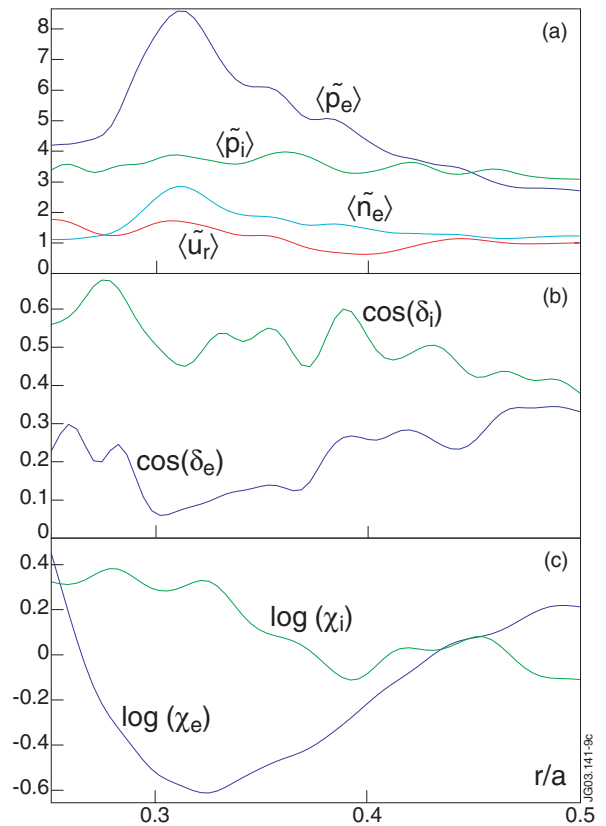


Figure 4. TRB simulations.

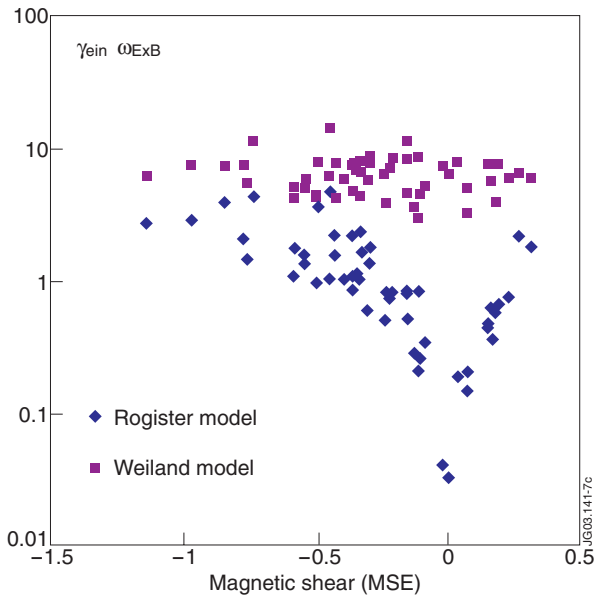


Figure 5.  $\gamma_{in}/\omega_{ExB}$  versus  $s$ .

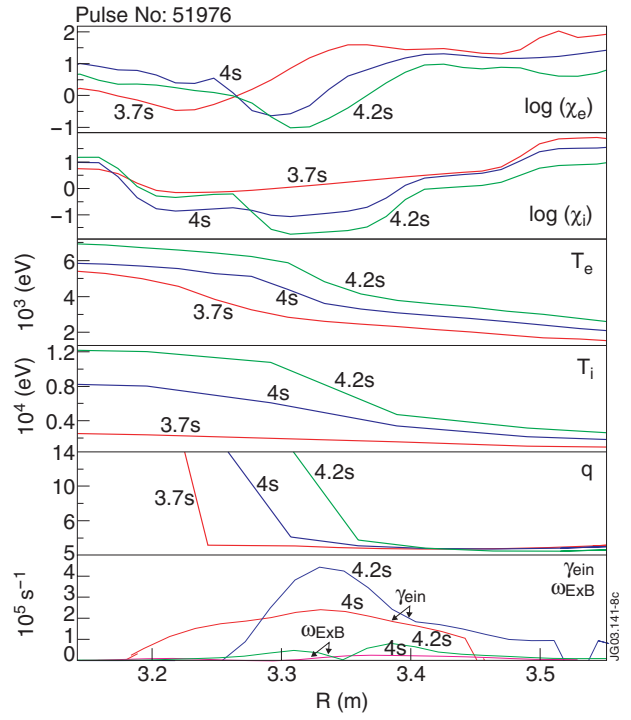


Figure 6. TRANSP modelling.

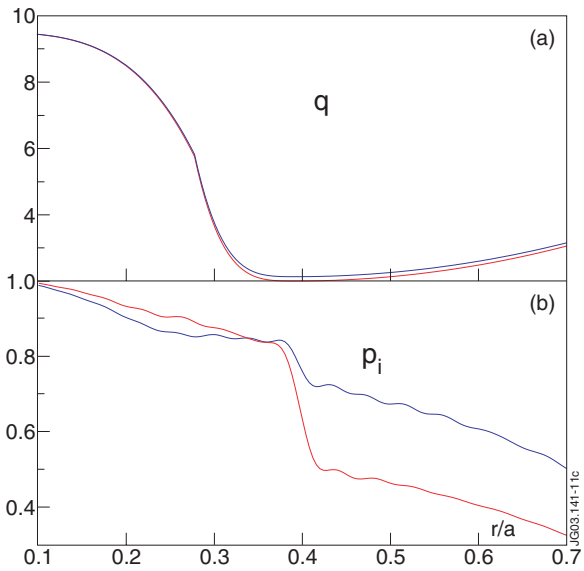


Figure 7. TRB simulations

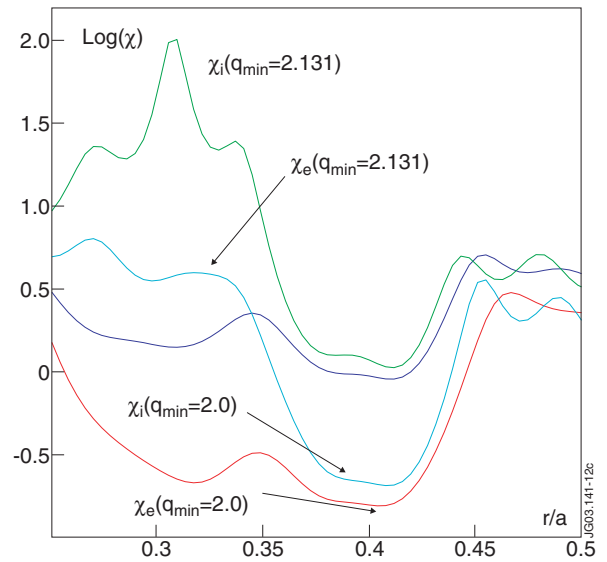


Figure.8 TRB simulations

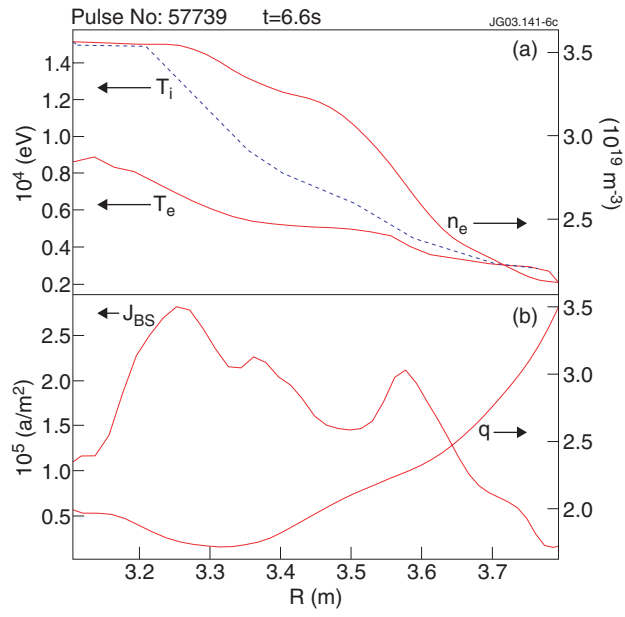


Figure 9. TRANSP modelling